Supporting Information

Monodispersed Ultramicroporous Semi-Cycloaliphatic Polyimides for Highly Efficient Adsorption of CO_2, H_2 and Organic Vapors

Jun Yan, Biao Zhang, and Zhonggang Wang*

State Key Laboratory of fine Chemicals, Department of Polymer Science and Materials, School of Chemical Engineering, Dalian University of Technology, Dalian 116024, China

Email: zgwang@dlut.edu.cn

Table S1. K_H, A_0, and Q_0 Values for CO_2 Adsorption in Cycloaliphatic sPIs

Sample	T/K	K_H/mol g^{-1} Pa^{-1}	A_0/ln(mol g^{-1} Pa^{-1})	Q_0/kJ/mol
sPI-1	273	2.105×10^{-7}	-15.376	31.3
	298	6.591×10^{-8}	-16.535	
sPI-2	273	2.841×10^{-7}	-15.074	31.4
	298	8.897×10^{-8}	-16.235	

Table S2. K_H, A_0, and Q_0 Values for H_2 Adsorption in Cycloaliphatic sPIs

Sample	T/K	K_H/mol g^{-1} Pa^{-1}	A_0/ln(mol g^{-1} Pa^{-1})	Q_0/kJ/mol
sPI-1	77	1.316×10^{-6}	-13.541	7.21
	87	3.601×10^{-7}	-14.837	
sPI-2	77	1.724×10^{-6}	-13.271	7.64
	87	4.402×10^{-7}	-14.636	

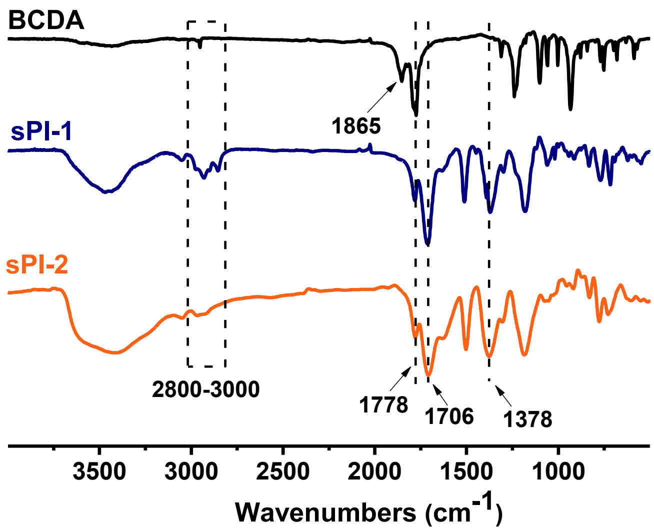

Figure S1. FT-IR spectra of dianhydride monomer BCDA and two polyimdes sPIs.

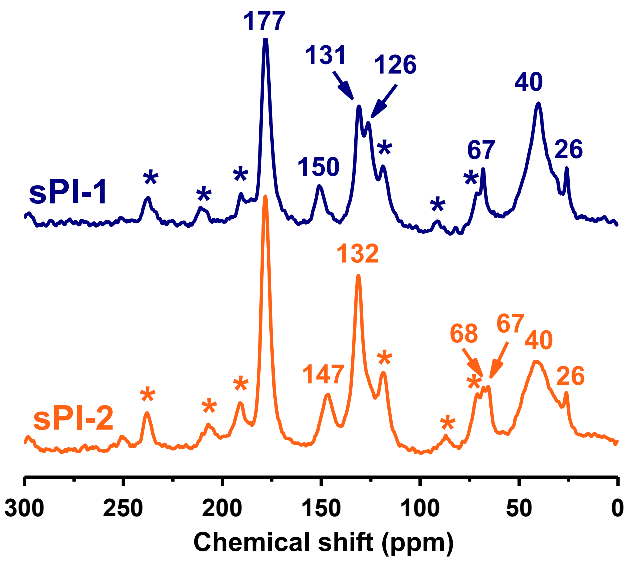

Figure S2. Solid-state ^{13}C CP/MAS NMR spectra of sPI-1and sPI-2. Asterisks (*) indicate peaks arising from spinning side bands.

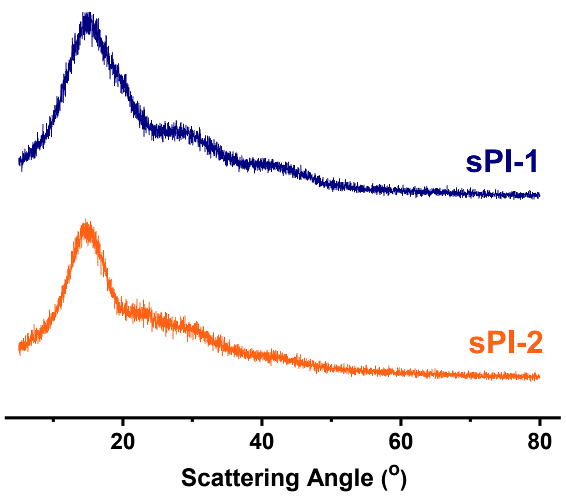

Figure S3. Wide angle X-ray diffractions of sPI-1 and sPI-2

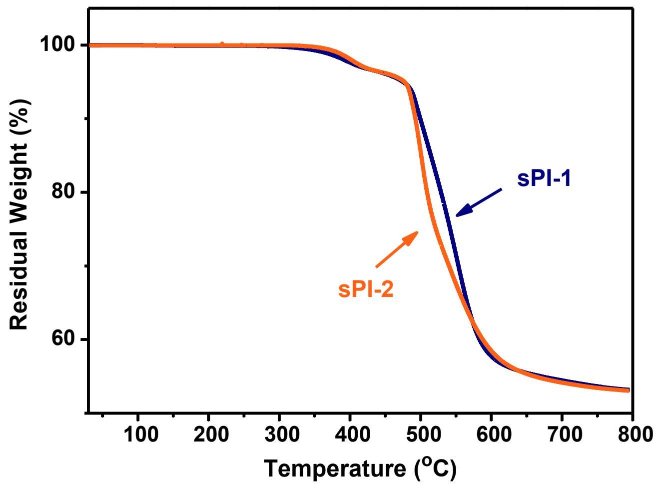

Figure S4. TGA curves of sPI-1 and sPI-2.

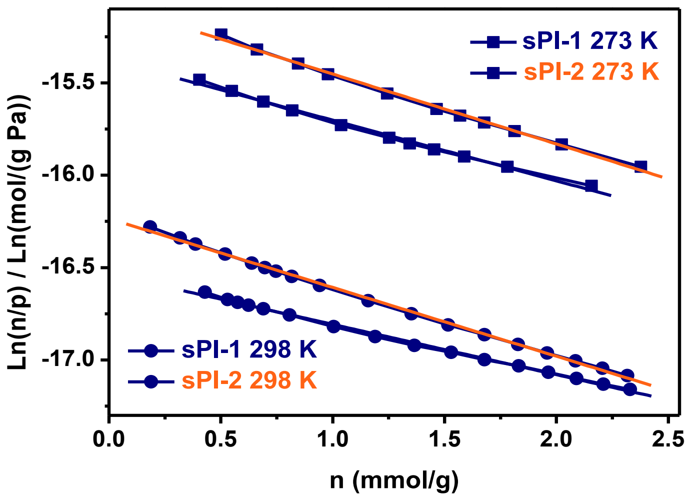

Figure S5. Virial plots of CO_2 for sPI-1 and sPI-2

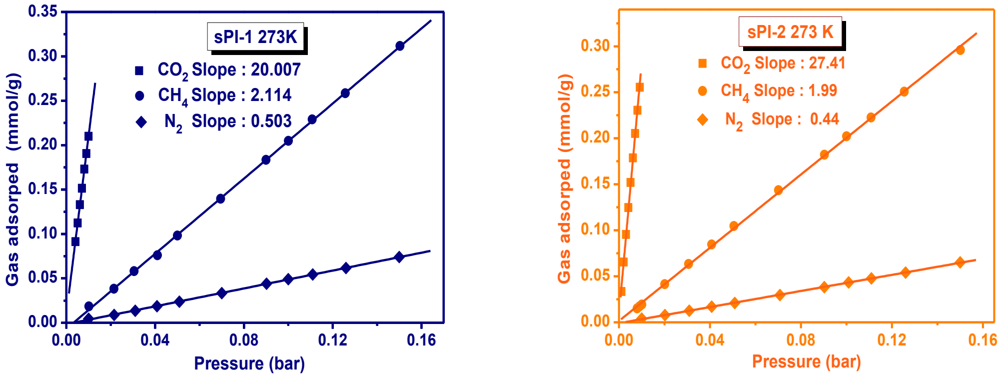

Figure S6. Adsorption isotherms of CO_2, CH_4 and N_2 at 273K for sPI-1 and sPI-2

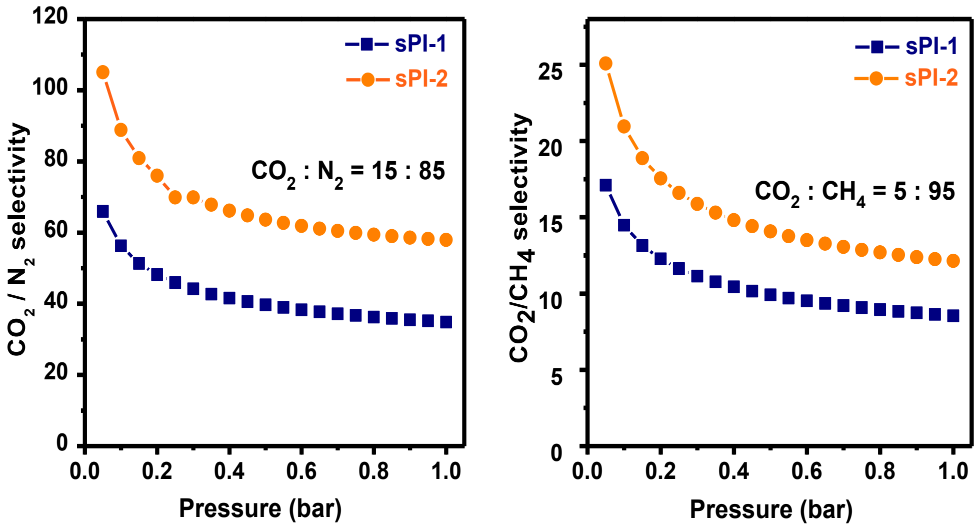

Figure S7. IAST selectivities for CO_2/N_2 and CO_2/CH_4 mixtures for sPI-1 and sPI-2 at 273 K.

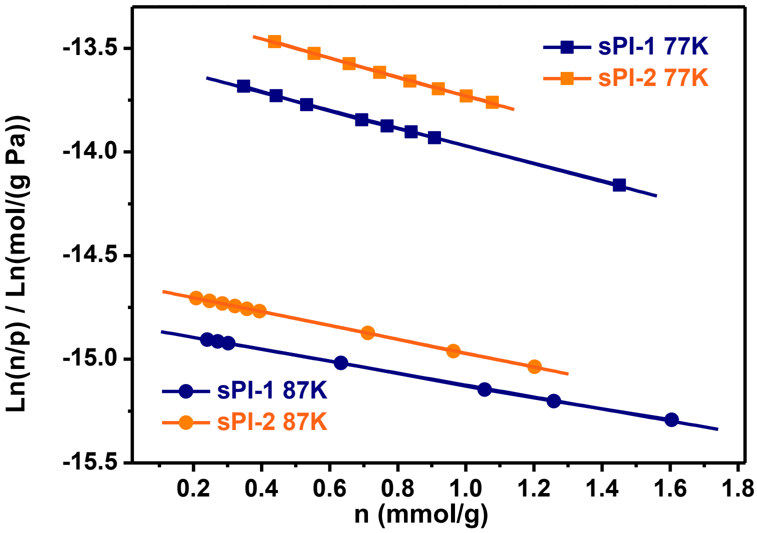

Figure S8. Virial plots of H_2 for sPI-1 and sPI-2